nature immunology

Interaction of the selectin ligand PSGL-1 with chemokines CCL21 and CCL19 facilitates efficient homing of T cells to secondary lymphoid organs

Krystle M Veerman[1,5], Michael J Williams[1,5], Kenji Uchimura[2,6], Mark S Singer[2], Jasmeen S Merzaban[1,6], Silvia Naus[1], Douglas A Carlow[1], Philip Owen[1], Jesús Rivera-Nieves[3], Steven D Rosen[2] & Hermann J Ziltener[1,4]

P-selectin glycoprotein ligand 1 (PSGL-1) is central to the trafficking of immune effector cells to areas of inflammation through direct interactions with P-selectin, E-selectin and L-selectin. Here we show that PSGL-1 was also required for efficient homing of resting T cells to secondary lymphoid organs but functioned independently of selectin binding. PSGL-1 mediated an enhanced chemotactic T cell response to the secondary lymphoid organ chemokines CCL21 and CCL19 but not to CXCL12 or to inflammatory chemokines. Our data show involvement of PSGL-1 in facilitating the entry of T cells into secondary lymphoid organs, thereby demonstrating the bifunctional nature of this molecule.

Immune surveillance requires that lymphocytes frequently home to secondary lymphoid organs (SLOs) to monitor for foreign antigens presented by antigen-presenting cells. The entry of blood-borne lymphocytes into lymph nodes is restricted to specialized postcapillary venules known as high endothelial venules (HEVs)[1]. To exit the blood vessels under the shear force of blood flow, lymphocytes undergo a complex multistep process that involves adhesive and chemotactic events and is characterized by tethering and rolling, followed by cell arrest and extravasation. Interaction of L-selectin on lymphocytes with its low-affinity ligand, 6-sulfo sialyl Lewis X, presented on peripheral node addressin (PNAd) expressed on HEVs, is an essential step in this cascade of events[2]. The relatively slow rolling induced by the L-selectin–PNAd interaction allows the lymphocytes sufficient time to initiate the second critical step in the homing cascade: responding to local chemokines presented on the lumenal aspect of HEVs[3]. The chemokines CCL21 and CCL19 are recognized as being central to this step[4,5]. Their interaction with the chemokine receptor CCR7, expressed on lymphocytes, induces the third crucial step of the cascade: activation of the integrin LFA-1 on lymphocytes[6]. Interaction of LFA-1 with its ligand ICAM-1 expressed on HEVs results in cell arrest, which is followed by immigration of cells into the lymph nodes[7,8]. Although naive T cells, central memory T cells and naive B cells all use the same adhesion cascade to enter lymph nodes from the blood[1], some differences do exist in the molecular requirements for homing to SLOs. Homing of naive T cells is most strongly affected by lack of CCL21 and CCL19 (ref. 5) or CCR7 (ref. 4), whereas homing of naive B cells is also dependent on CXCL12 and CXCR4 (ref. 9) and involves less L-selectin[10,11].

Naive T cells that have entered the SLOs and encounter dendritic cells presenting their cognate antigen will undergo clonal expansion, become effector cells and leave the lymphoid organ to eventually re-enter the bloodstream[1]. A similar highly regulated multistep adhesion cascade also controls the recruitment of effector cells from the bloodstream to inflamed tissues, with a notable difference being that the first crucial step of rolling and tethering is often mediated by the interaction of appropriately glycosylated P-selectin glycoprotein ligand-1 (PSGL-1) on the activated lymphocyte with P-selectin and/or E-selectin expressed on activated endothelial cells lining the postcapillary venules of inflamed tissue[12]. It was previously thought that distinct arrays of molecules were required for the homing of naive cells to SLOs versus the recruitment of inflammatory cells. However, the known function of PSGL-1 in the recruitment of effector cells to sites of inflammation[13] has been extended to include homing of thymic progenitors to the thymus[14], thereby establishing the involvement of PSGL-1 in homing in noninflammatory conditions. Here we provide evidence that PSGL-1 is a bifunctional molecule that has, in addition to its established proadhesive function, a chemotaxis-enhancing function required for the efficient homing of resting T cells to SLOs through a mechanism that is independent of the interaction of PSGL-1 with selectins.

[1]The Biomedical Research Centre, University of British Columbia, Vancouver, British Columbia V6T 1Z3, Canada. [2]Department of Anatomy and Program in Immunology, University of California, San Francisco, San Francisco, California 94143-0452, USA. [3]Digestive Health Center of Excellence, University of Virginia Health Sciences Center, Charlottesville, Virginia 22908 USA. [4]Department of Pathology and Laboratory Medicine, University of British Columbia, Vancouver, British Columbia V6T 1Z3, Canada. [5]These authors contributed equally to this work. [6]Present addresses: National Institute for Longevity Sciences, 36-3 Gengo, Morioka, Obu, Aichi 474-8511, Japan (K.U.), and Harvard Institutes of Medicine, Boston, Massachusetts 02115, USA (J.S.M.). Correspondence should be addressed to H.J.Z. (hermann@brc.ubc.ca).

Received 16 November 2006; accepted 8 March 2007; published online 1 April 2007; doi:10.1038/ni1456

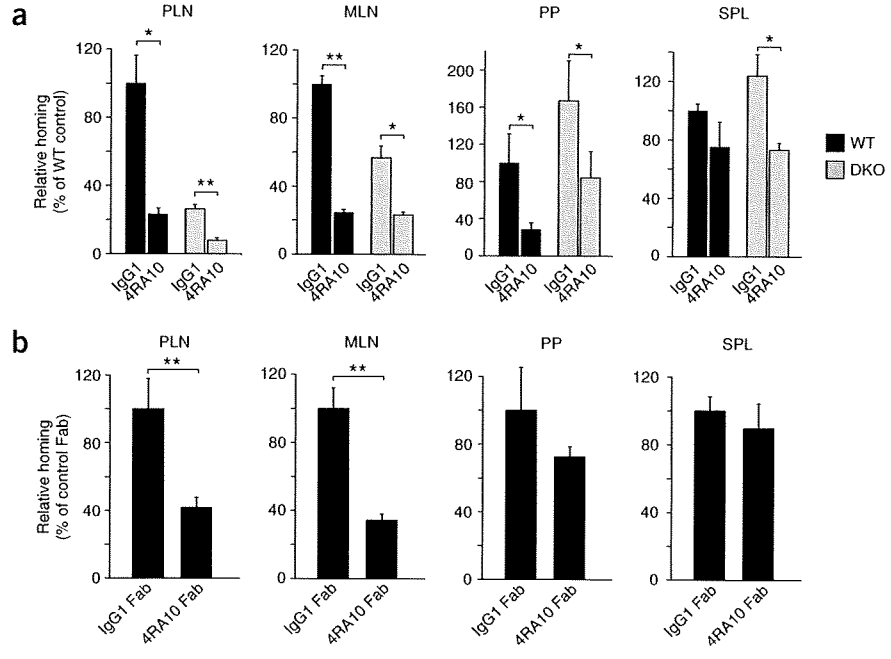

Figure 1 PSGL-1 is required for efficient homing of lymphocytes to SLOs. **(a)** Flow cytometry to assess homing of lymphocytes after treatment with mAb 4RA10. Cells from CD-1 mouse donors were labeled with CMFDA and treated with mAb 4RA10 or control IgG1 before injection into the tail veins of age-matched C57BL/6 wild-type recipient mice (WT; $n = 3$ mice) or recipient mice lacking both GlcNAc6ST-1 and GlcNAc6ST-2 (DKO; $n = 3$ mice); absolute numbers of $CMFDA^+$ cells from recipient peripheral lymph nodes (PLN), mesenteric lymph nodes (MLN), Peyer's patches (PP) and spleen (SPL) were determined 1 h after injection. **(b)** Flow cytometry to assess homing of lymphocytes after treatment with Fab fragments of mAb 4RA10. Cells from CD-1 mouse donors were labeled with CMFDA and treated with Fab fragments of mAb 4RA10 or IgG1 before injection into the tail veins of C57BL/6 wild-type recipient mice ($n = 3$ mice); $CMFDA^+$ cells in recipient SLOs were analyzed 1 h later. Raw data for *in vivo* homing experiments are in **Supplementary Table 1** online. *, $P < 0.05$, and **, $P < 0.001$, mAb 4RA10 versus IgG1 (Student's *t*-test). Data are mean (+ s.d.) percent cells relative to wild-type IgG1 control **(a)** or wild-type IgG1 Fab control **(b)**; and are representative of at least three independent experiments **(a)** or are representative of two independent experiments **(b)**.

RESULTS

Efficient homing of T cells to SLOs requires PSGL-1

While analyzing parabiotic mice to delineate the function of PSGL-1 in thymic progenitor homing[14], we noted that T cells lacking PSGL-1 expression were approximately 50% less represented in lymph nodes than were T cells expressing PSGL-1, whereas in the spleen, both T cell types were present in comparable numbers. Those findings raised the possibility that T cell–expressed PSGL-1 may be required for the efficient homing of T cells to lymph nodes. To further investigate that issue, we tested whether antibody blockade of PSGL-1 would affect the short-term homing of lymphocytes to SLOs. Treatment of lymphocytes with monoclonal antibody (mAb) 4RA10 to PSGL-1 significantly reduced short-term homing to SLOs (**Fig. 1a**). Homing to peripheral lymph nodes was reduced by 77% ± 16% ($P = 0.0013$), homing to mesenteric lymph nodes was reduced by 75% ± 5% ($P = 0.000014$) and homing to Peyer's patches was reduced by 71% ± 6.7% ($P = 0.018$); however, homing to spleen was reduced by 25% ± 17% and this result did not achieve statistical significance ($P = 0.07$). Mice deficient in the *N*-acetylglucosamine-6-*O*-sulfotransferases GlcNAc6ST-1 and GlcNAc6ST-2 lack functional PNAd and have much less homing of lymphocytes to lymph nodes, as their HEVs cannot synthesize the sialyl 6-sulfo $Lewis^x$ determinants required for L-selectin binding[15,16]. Residual homing was inhibited by mAb 4RA10 to the same degree in mice deficient in both sulfotransferases and in wild-type mice ($P < 0.05$), indicating that PSGL-1-dependent homing occurred in the presence or absence of functional PNAd. Monovalent Fab fragments of mAb 4RA10 also inhibited the short-term homing of lymphocytes to SLOs, excluding the possibility that agglutination of lymphocytes or Fc-receptor mediated events were responsible for the reduced homing (**Fig. 1b**). These Fab fragments inhibited homing to peripheral and mesenteric lymph nodes by 65% ± 3.6% ($P = 0.000048$) and 58% ± 6% ($P = 0.0009$), respectively. Homing to Peyer's patches and spleen was reduced by 28% ± 6% ($P = 0.08$) and 11% ± 14.8% ($P = 0.27$), respectively, indicating trends lacking statistical significance.

To further corroborate the idea that PSGL-1 is involved in homing to SLOs, we did competitive short-term homing assays with mixtures of fluorescence-labeled lymphocytes from PSGL-1-null and wild-type mice. The results (**Fig. 2a**) closely paralleled the mAb inhibition studies. Homing of PSGL-1-null lymphocytes to lymph nodes was 49% ± 4.5% less than that of wild-type ($P = 0.0000000083$), whereas homing to Peyer's patches was 35% ± 10.7% less ($P = 0.000069$) and homing to the spleen was 10% ± 4.7% less ($P = 0.0014$). In the peripheral blood, the numbers of wild-type and PSGL-1-null lymphocytes were similar ($P = 0.28$). Control experiments with wild-type lymphocytes showed that the fluorescent labels used did not affect the SLO-homing properties of lymphocytes (**Supplementary Fig. 1** online).

To determine whether PSGL-1 conferred on all the main lymphocyte subsets efficient homing to SLOs, we monitored the PSGL-1-dependent homing of B cells and of T cell subsets in the competitive short-term homing assay. Homing of B cells to SLOs was not affected by PSGL-1 status ($P = 0.34$), as the ratio of wild-type to PSGL-1-null B cells that had migrated into peripheral lymph nodes remained identical to the ratio in peripheral blood (**Fig. 2b**). In contrast to its effect on the homing of B cells, lack of PSGL-1 resulted in a similar lower lymph node–homing efficiency for $CD4^+$ and $CD8^+$ T cells of both the naive ($CD44^{lo}$) and central memory ($CD44^{hi}$) phenotype ($P < 0.0003$).

PSGL-1 effect is independent of selectin interactions

PSGL-1 is known to interact with all three selectins[17]. Therefore, one possibility was that PSGL-1 binds to hitherto undetectable amounts of E-selectin and/or P-selectin expressed on HEVs. Alternatively, it was possible that T cells adhering to HEVs through L-selectin–PNAd interactions bind other lymphocytes by secondary tethering through an L-selectin–PSGL-1 interaction[18]. To determine whether E-selectin or P-selectin interactions were involved, we did competitive lymphocyte homing experiments with E-selectin-null or P-selectin-null recipient mice, with the expectation that the competitive advantage of wild-type lymphocytes would be lost if the vascular selectin were required. However, the homing advantage of wild-type over

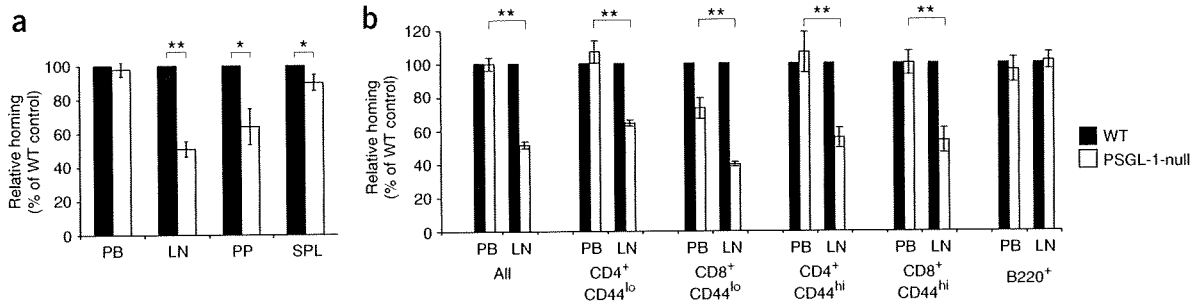

Figure 2 The effect of PSGL-1 on homing to SLOs is restricted to resting T lymphocytes. (**a**) Competitive *in vivo* short-term homing of lymphocytes from C57BL/6 wild-type and PSGL-1-null mouse donors, labeled with CFDA-SE or CTO and injected intravenously into C57BL/6 wild-type recipient mice; relative numbers of labeled lymphocytes in recipient peripheral blood (PB), lymph nodes (LN), Peyer's patches (PP) and spleen (SPL) were determined by flow cytometry after 1 h. (**b**) Flow cytometry of lymphocyte subsets among CFDA-SE-labeled C57BL/6 wild-type lymphocytes and GFP-transgenic PSGL-1-null lymphocytes injected intravenously into wild-type recipient mice and assessed 1 h later in recipient peripheral blood and lymph nodes. Raw data for *in vivo* homing experiments are in **Supplementary Table 2** online. *, $P < 0.05$, and **, $P < 0.001$ (Student's *t*-test; **a**, $n = 5$; **b**, $n = 4$). Data are mean (+ s.d.) percent cells relative to wild-type and are representative of five (**a**) or three (**b**) independent experiments.

PSGL-1-null lymphocytes was maintained in both E-selectin-deficient and P-selectin-deficient recipient mice (**Fig. 3a,b**). These data rule out the possibility of involvement of selectin binding. As the interaction of PSGL-1 with L-selectin and P-selectin is dependent on activity of the core 2 glycosyltransferase 'C2GlcNAcT-I'[19,20], we did competitive homing assays with lymphocytes from C2GlcNAcT-I-null and wild-type donors. Both populations homed equivalently to the various SLOs (**Supplementary Fig. 2** online), whereas in competition between lymphocytes lacking C2GlcNAcT-I alone and lymphocytes lacking both C2GlcNAcT-I and PSGL-1 in recipient mice lacking both C2GlcNAcT-I and PSGL-1, the donor cells lacking PSGL-1 remained at a disadvantage (**Supplementary Fig. 2**), challenging the idea of involvement of L-selectin or P-selectin. Finally, competition in E-selectin-null recipient mice between lymphocytes lacking C2GlcNAcT-I alone and lymphocytes lacking both C2GlcNAcT-I and PSGL-1 allowed simultaneous exclusion of the possibility of involvement of all three selectins in the short-term homing assay (**Fig. 3c**). Again, cells lacking PSGL-1 remained at a disadvantage, demonstrating that our inability to show involvement of selectins was not due to selectin redundancy. In summary, it is unlikely that interaction of PSGL-1 with one or more selectins was the mechanism supporting the homing of T cells to SLOs; thus, we explored other possibilities, including the involvement of chemokines.

PSGL-1-null T cells have lower chemotactic responses

The chemokines CCL21 and CCL19 are constitutively produced in lymph nodes[21] and are presented on the surfaces of HEVs, most likely through an association with glycosaminoglycans[6]. Loss of CCL19 and CCL21 is associated with a defect in the migration of T cells to SLOs, which demonstrates the importance of these chemokines in lymphocyte homing[5]. Studies have shown that a small subset of chemokines, including CCL21 and CCL27, can bind the amino (N) terminus of human PSGL-1 by a tyrosine-sulfation-dependent interaction[22]. We therefore sought to determine whether lack of PSGL-1 would alter the chemotactic response of lymphocytes to CCL21. In competitive transwell chemotaxis assays, PSGL-1-null lymphocytes migrated about 30% less effectively than wild-type lymphocytes in response to CCL21, and the attenuated chemotactic response was present over a wide range of CCL21 concentrations (**Fig. 4a**; $P < 0.005$). As loss of the abundant and heavily glycosylated molecule PSGL-1 might conceivably alter the chemotactic response of lymphocytes in a non-specific way, we sought to determine whether lack of CD43, a mucin expressed in high abundance on lymphocytes[23], also affected their chemotactic response. Loss of CD43 did not inhibit the response of cells to CCL21; instead, cells lacking CD43 seemed to migrate somewhat more efficiently than wild-type cells (5–8% increase over wild-type; **Fig. 4b**). Because our *in vivo* homing data showed that the effect

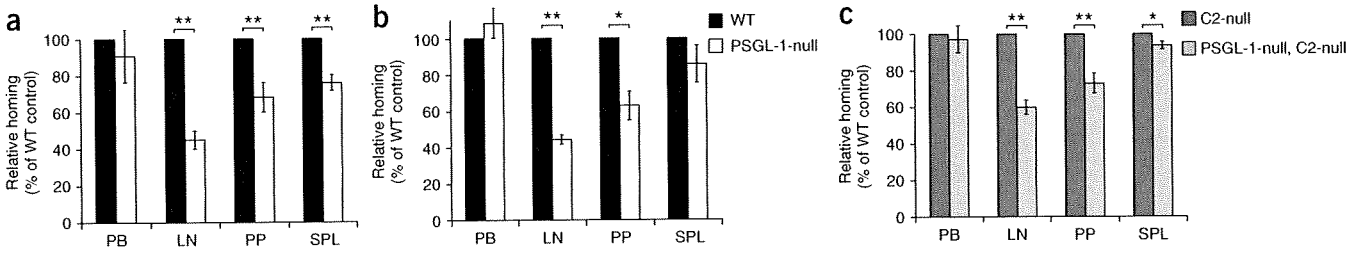

Figure 3 The contribution of PSGL-1 in the homing to SLOs is not dependent on its interaction with selectins. (**a,b**) Competitive *in vivo* short-term homing of lymphocytes from C57BL/6 wild-type and PSGL-1-null mouse donors, labeled with CFDA-SE or CTO and injected intravenously into E-selectin-null recipients (**a**; $n = 4$ mice) or P-selectin-null recipients (**b**; $n = 3$ mice). Lymph nodes, $P = 0.00000052$ (**a**) or $P = 0.0000029$ (**b**); Peyer's patches, $P = 0.0002$ (**a**) or $P = 0.0014$ (**b**); spleen, $P = 0.000028$ (**a**) or $P = 0.075$ (**b**); peripheral blood, $P = 0.24$ (**a**) or $P = 0.13$ (**b**), all wild-type versus PSGL-1-null donor (Student's *t*-test). (**c**) Flow cytometry of the relative number of lymphocytes lacking C2GlcNAcT-I (C2-null) and lymphocytes lacking both PSGL-1 and C2GlcNAcT-I (PSGL-1-null, C2-null), labeled with CFDA-SE or CTO and injected into E-selectin-null recipient mice ($n = 4$ mice), detected in recipient peripheral blood ($P = 0.075$), lymph nodes ($P = 0.0000021$), Peyer's patches ($P = 0.00016$) and spleen ($P = 0.002$). *, $P < 0.05$, and **, $P < 0.001$ (Student's *t*-test). Raw data for *in vivo* homing experiments are in **Supplementary Table 3** online. Data are mean (+ s.d.) percent cells relative to wild-type and are representative of at least three independent experiments.

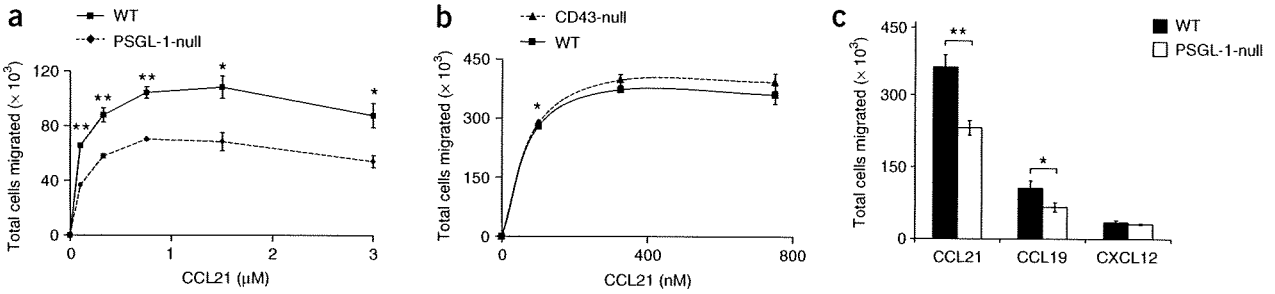

Figure 4 PSGL-1 is required for efficient chemotaxis to CCL21 and CCL19 but not to CXCL12. (**a**) Competitive *in vitro* chemotaxis assays of lymphocytes from C57BL/6 wild-type and GFP-transgenic PSGL-1-null mouse donors (**a**) or wild-type and CD43-null mice (**b**); cells were incubated for 1 h in transwells with varying concentrations of CCL21. *, $P < 0.05$, and **, $P < 0.001$ (Student's *t*-test): 100 nM, $P = 0.0000066$, 375 nM, $P = 0.000071$, 750 nM, $P = 0.00016$, 1.5 μM, $P = 0.0029$, and 3 μM, $P = 0.0042$ (**a**); 100 nM, $P = 0.02$, 375 nM, $P = 0.06$, and 750 nM, $P = 0.17$ (**b**). (**c**) *In vitro* chemotaxis assays of purified T lymphocytes from wild-type and GFP-transgenic PSGL-1-null donors; cells were incubated for 2–3 h in transwells with 200 nM CCL21, CCL19 or CXCL12. *, $P < 0.05$, and **, $P < 0.001$ (Student's *t*-test). Data are mean (± s.d.) number of cells recovered from the lower chamber, after subtraction of the number of cells migrating in absence of chemotactic agent ($n = 3$ (**a**,**b**) or 4 (**c**) transwell replicates per point), and are representative of at least three independent experiments.

of PSGL-1 was restricted to T cells of both the naive and central memory types, we used purified T cells to confirm the results obtained above with unfractionated lymphocytes. We also evaluated two additional chemokines, CCL19 and CXCL12, also known to be involved in lymphocyte homing[24,25], in the transwell chemotaxis assay. Wild-type and PSGL-1-null T cells migrated equally toward CXCL12 ($P = 0.11$), whereas the response to CCL19 was approximately 30% weaker for T cells lacking PSGL-1, as was the case for CCL21 ($P = 0.004$ and $P = 0.002$, respectively; **Fig. 4c**). Thus, PSGL-1 enhanced the chemotactic response of T cells to the two SLO chemokines CCL21 and CCL19 but not to CXCL12.

CCL21 binds T cells in a PSGL-1-dependent way

Our data indicated that binding of chemokine to PSGL-1 might be the underlying cause of the enhanced chemotactic responses of T cells. If so, CCL21 and possibly CCL19 would bind T cells not only by means of their cognate chemokine receptor CCR7 (ref. 26) and cell surface–expressed glycosaminoglycans, including heparan sulfate and chondroitin sulfate[27], but also by means of PSGL-1. To demonstrate a chemokine–PSGL-1 interaction, we immobilized decreasing amounts of CCL21 or control CXCL12 on nitrocellulose and 'probed' with a fusion protein of PSGL-1 and immunoglobulin G (IgG). With this approach, we found that PSGL-1 bound immobilized CCL21 but not CXCL12 (**Fig. 5a**). To directly assess the interaction of CCL21 with PSGL-1 expressed on lymphocytes, we synthesized mouse CCL21 biotinylated at the N terminus. Staining lymphocytes with this reagent showed that both $CD4^+$ and $CD8^+$ T cells bound CCL21 with a biphasic pattern. Notably, $CCL21^{hi}$ $CD4^+$ and $CD8^+$ T cells from wild-type mice bound considerably more CCL21 than the corresponding T cells from PSGL-1-null mice (**Fig. 5b**). In contrast, binding of CCL21 to B cells produced a relatively strong monophasic signal that was not affected by PSGL-1 expression; PSGL-1 expression was much lower on B cells than on T cells (**Supplementary Fig. 3** online). The '$CCL21^{dim}$' cells represent T cells that have internalized CCL21. The conditions we used for the CCL21 binding assay were similar to those used for chemotaxis assay and thus allowed chemokine internalization. We also

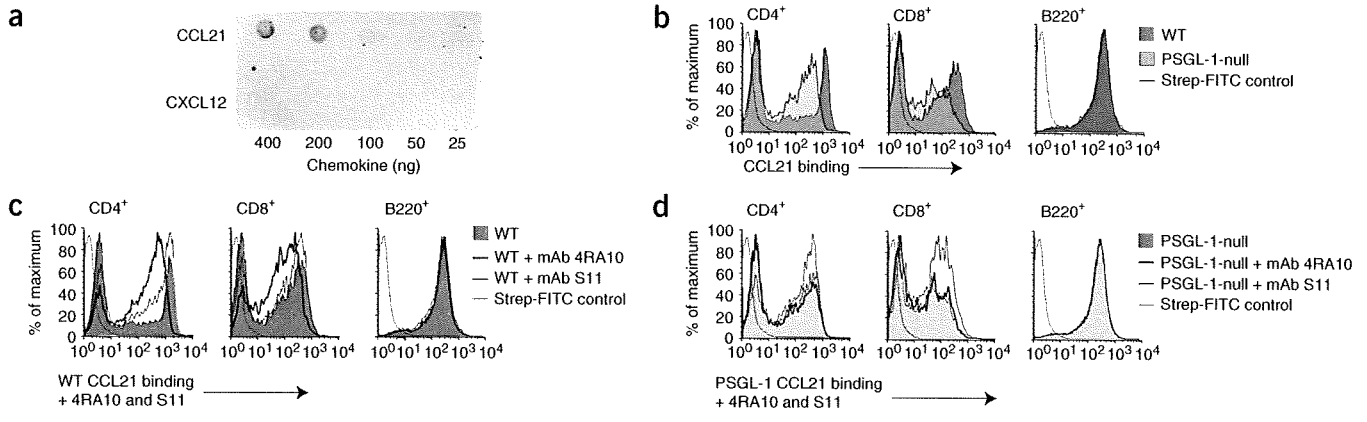

Figure 5 PSGL-1 binds CCL21. (**a**) Detection of CCL21 and CXCL12 immobilized on a nitrocellulose membrane with a PSGL-1–human IgG1 chimera and 'probed' with fluorescent anti–human IgG. (**b**) Flow cytometry of wild-type and PSGL-1-null lymphocytes incubated for 2 h with a mixture of biotin-CCL21 and fluorescein isothiocyanate–streptavidin (Strep-FITC), then co-stained with anti-CD4, anti-CD8 or anti-B220. (**c**,**d**) Flow cytometry of wild-type lymphocytes (**c**) and PSGL-1-null lymphocytes (**d**) incubated for 30 min with mAb 4RA10 (to PSGL-1) or mAb S11 (to CD43) before 2 h of incubation with fluorescein isothiocyanate–CCL21 followed by co-staining with anti-CD4, anti-CD8 or anti-B220. Fluorescein isothiocyanate–streptavidin staining without chemokine, negative control. Data are representative of four independent experiments.

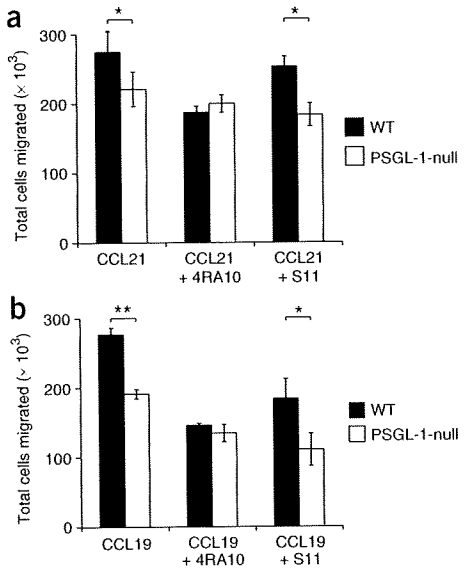

Figure 6 Chemotactic advantage of wild-type over PSGL-1-null T cells is blocked by mAb 4RA10 (to PSGL-1). Competitive *in vitro* transwell chemotaxis assay of the migration of C57BL/6 wild-type T cells and GFP-labeled PSGL-1-null T cells toward 200 nM CCL21 (**a**) or 200 nM CCL19 (**b**) after incubation of cells with mAb 4RA10 (to PSGL-1) or mAb S11 (to CD43). *, $P < 0.05$, and **, $P < 0.001$ (Student's *t*-test). Data are mean (± s.d.) number of cells recovered from the lower chamber after 2 h of incubation, after subtraction of the number of cells migrating in absence of chemotactic agent ($n = 4$ transwell replicates per point), and are representative of three independent experiments.

did CCL21 binding studies in the presence of sodium azide to prevent chemokine internalization. As expected, binding of CCL21 to T cells was monophasic in presence of sodium azide. However, although the difference in the binding of CCL21 to wild-type versus PSGL-1-null cells was still present, it was much less, as was the inhibition of CCL21 binding by antibody to PSGL-1 (anti-PSGL-1; **Supplementary Fig. 4** online).

The binding of mAb 4RA10 has been mapped to the N terminus of PSGL-1, a region also important for the binding of P-selectin and chemokines[22,28]. The binding of CCL21 to $CD4^+$ and $CD8^+$ T cells from wild-type mice was reduced with mAb 4RA10, such that it was similar to that of PSGL-1-null T cells (**Fig. 5c**), whereas the binding of CCL21 to B cells (**Fig. 5c**) or PSGL-1-deficient T cells (**Fig. 5d**) was not affected by mAb 4RA10. Pretreatment of cells with a mAb (S11) to CD43, another leukocyte mucin, had no effect on the CCL21 binding profiles. These results collectively demonstrated direct interaction of CCL21 with PSGL-1 expressed on $CD4^+$ and $CD8^+$ T cells.

Figure 7 Core 2 *O*-glycan branch formation on PSGL-1 causes loss of enhanced chemotaxis on activated T cells. (**a**) Competitive *in vitro* transwell chemotaxis assay of the migration of C57BL/6 wild-type and PSGL-1-null lymphocytes toward 200 nM CCL21, CXCL11 or CXCL9, 4 d after cells were activated with concanavalin A. (**b**) Chemotactic responses to 200 nM CCL21, of wild-type versus PSGL-1-null lymphocytes and of lymphocytes lacking C2GlcNAcT-I versus lymphocytes lacking both PSGL-1 and C2GlcNAcT-I, before activation (left; Lymph node cells) and 4 d after activation with concanavalin A (right; Activated T cells). *, $P < 0.05$, and **, $P < 0.001$ (Student's *t*-test; $n = 4$). Data are mean (± s.d.) number of cells recovered from the lower chamber after 2 h of incubation, after subtraction of the number of cells migrating in absence of chemotactic agent, and are representative of three independent experiments.

Anti-PSGL-1 blocks the PSGL-1-enhanced chemotaxis

The inhibition of the CCL21–PSGL-1 interaction by treatment with mAb 4RA10 suggested that this mAb might inhibit the chemotactic advantage associated with T cells expressing PSGL-1 and responding to CCL21 or CCL19. To test that hypothesis, we added neutralizing amounts of mAb 4RA10 to the competitive chemotaxis assay. This eliminated the chemotactic advantage of wild-type cells in response to both CCL21 and CCL19 ($P = 0.91$ and $P = 0.84$, respectively; **Fig. 6**). In contrast, PSGL-1-null cells remained at a chemotactic disadvantage (CCL21, $P = 0.02$; CCL19, $P = 0.01$) in the presence of mAb S11 (to CD43). Thus, mAb 4RA10 abrogated the PSGL-1-mediated chemotactic advantage, whereas mAb S11 did not.

PSGL-1-enhanced chemotaxis is lost on activated T cells

Activated T cells upregulate the chemokine receptor CXCR3 (ref. 29) and become responsive to the inflammatory chemokines CXCL9, CXCL10 and CXCL11 (also called Mig, IP-10 and I-TAC). Analysis of T cells activated by the mitogen concanavalin A showed that chemotactic migration of activated PSGL-1-null T cells toward CXCL9 and CXCL11 was not lower; indeed these cells showed a trend to migrate better than wild-type cells (20–40% increase over wild-type cells; $P = 0.06$ and $P = 0.31$, respectively; **Fig. 7a**). Activated T cells remained responsive to CCL21 (ref. 30) but migrated equivalently to this chemokine with or without PSGL-1 ($P = 0.30$; **Fig. 7a**), suggesting that the PSGL-1-enhanced migration to CCL21 and CCL19 does not apply to all differentiation states of T cells.

T cell activation results in the coordinated upregulation of several glycosyltransferases required for functional P-selectin ligand formation on PSGL-1 (ref. 17). Expression of core 2 *O*-glycan–branched sialyl Lewis X on Thr17 as well as sulfation of Tyr13 on the N terminus of mouse PSGL-1 are essential for the binding of P-selectin[31]. Loss of the CCL21–PSGL-1 effect on activated T cells could thus be due to upregulation of core 2–branched sialyl Lewis X on Thr17, which may block the putative CCL21 interaction with sulfated Tyr13 and/or sulfated Tyr15 on PSGL-1 (ref. 22). To test for such a function for core 2 *O*-glycans, we determined whether T cells lacking C2GlcNAcT-I maintained their PSGL-1-linked chemotactic advantage after activation. We therefore compared the chemotactic response of T cells deficient in C2GlcNAcT-I with that of T cells lacking both C2GlcNAcT-I and PSGL-1. Consistent with our short-term homing results, resting T cells from donors lacking both C2GlcNAcT-I and PSGL-1 were at a chemotactic disadvantage relative to those from

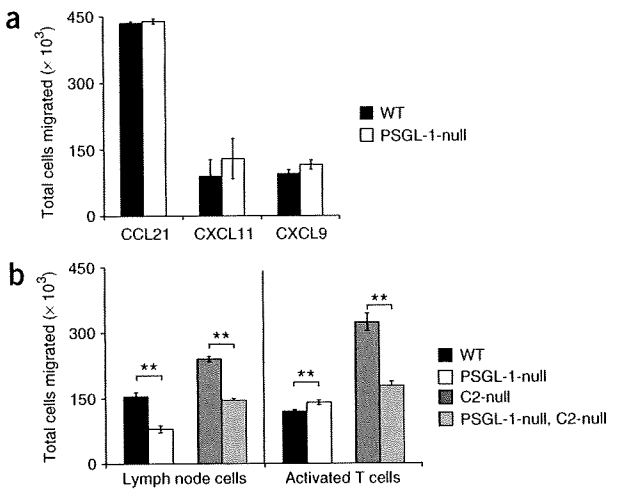

donors lacking only C2GlcNAcT-I ($P = 0.00000023$; **Fig. 7b**). However, contrary to our finding with activated C2GlcNAcT-I-sufficient T cells, activated C2GlcNAcT-I-null T cells maintained their advantage over activated T cells lacking both C2GlcNAcT-I and PSGL-1 ($P = 0.000013$; **Fig. 7b**); in fact, the activated C2GlcNAcT-I-null T cells migrated twofold better than activated T cells from either wild-type or PSGL-1-null donors. Thus, the core 2 *O*-glycan branch seemed to interfere with the postulated CCL21–PSGL-1 interaction.

DISCUSSION

Our data have demonstrated a previously unrecognized function of PSGL-1 in the homing of T cells to SLOs by enhancing chemotactic responses to the SLO chemokines CCL21 and CCL19. The effect of PSGL-1 on homing to SLOs was restricted to naive and central memory T cells and did not extend to B cells, which express less PSGL-1 and are much less dependent on CCL21 or CCL19 for homing to SLOs than are T cells[9]. The observed lower chemotactic response of PSGL-1-null T cells to CCL21 and CCL19 was not due to complete loss of chemotactic responsiveness of specific T cell subsets. Given that loss of PSGL-1 expression similarly affects the homing of all T cell subsets to SLOs, we propose that loss of PSGL-1 expression results in an overall lower migratory response of T cells.

PSGL-1, originally identified as a ligand for P-selectin, can bind all three selectins and has a central proadhesive function in many inflammatory settings[17]. The possibility of involvement of any of the selectins in the mechanism of action driving the enhanced homing of T cells to SLOs can be ruled out based on our competitive homing experiments using selectin-deficient recipients and/or C2GlcNAcT-I-null donor lymphocytes. Furthermore, resting T cells (naive and central memory T cells) do not have C2GlcNAcT activity and consequently do not express PSGL-1 capable of binding P-selectin and L-selectin.

The mechanism by which PSGL-1 functions in its chemotaxis-enhancing capacity is unclear at present. The findings of inhibition of *in vivo* lymphocyte homing by blockade with mAb 4RA10, inhibition of the binding of CCL21 to PSGL-1 by mAb 4RA10, and mAb 4RA10–mediated abrogation of the wild-type chemotactic advantage over PSGL-1-null T cells are consistent with a functional interaction between PSGL-1 and CCL21 or CCL19. It is likely that such an interaction would require the N-terminal tyrosine sulfates of mouse PSGL-1, as is the case for the binding of CCL27 to human PSGL-1 (ref. 22). The binding of CCL21 and/or CCL19 to PSGL-1 on the lymphocyte might precede the chemokine-CCR7 interaction on the same cell in a 'pass-on' process. The physiological utility of this CCL21–PSGL-1 or CCL19–PSGL-1 interaction may be to capture chemokine, thereby counteracting a rapid loss that might otherwise occur in the bloodstream during transfer from the apical surface of HEVs to the rolling lymphocyte. PSGL-1 is a highly extended mucin[32] localized on microvilli[33] and might be well adapted for rapid and efficient transfer of the chemokine between the interacting cells. Alternatively, the CCL21–PSGL-1 or CCL19–PSGL-1 interaction may induce signaling by means of PSGL-1 (refs. 34,35) and actively contribute to an enhanced chemotactic response.

The L-selectin required by naive T cells to enter SLOs is down-regulated once T cells become activated, thus preventing activated T cells from re-entering SLOs. Notably, analysis of transgenic mice expressing 'non-sheddable' L-selectin has indicated that in addition to shedding of L-selectin, a second mechanism might exist that prevents re-entry of activated T cells into SLOs, as activated T cells expressing 'non-sheddable' L-selectin migrate less efficiently into lymph nodes than the corresponding naive T cells[36]. The PSGL-1-enhanced chemotaxis described here could be the basis of such a second mechanism, as the effect was lost in a core 2 *O*-glycan–dependent way on activated T cells. T cell activation–induced upregulation of core 2 *O*-glycan–branched sialyl Lewis X on Thr17 located on the N terminus of PSGL-1 may thus serve a dual purpose: first, to support the formation of functional selectin ligands, enabling trafficking of these cells to sites of inflammation, and second, to limit responses to chemokines such as CCL21 and CCL19, which in concert with L-selectin shedding would prevent activated T cells from re-entering SLOs.

The implications of the absence of PSGL-1 and of compromised homing to SLOs on normal immune function are not apparent at present and need to be explored in PSGL-1-deficient animals. Analysis by the Consortium for Functional Glycomics has shown that immunoglobulin production is decreased in PSGL-1-deficient mice in response to immunization with the T cell–dependent antigen keyhole limpet hemocyanin (http://www.functionalglycomics.org/glycomics/publicdata/phenotyping.jsp).Whether this effect is due to reduced homing of T cells to SLOs, however, remains to be determined.

The functional interaction of PSGL-1 with homing chemokines shown here substantially expands the recognized functional scope of this molecule. Our findings may stimulate reconsideration of previous analyses using PSGL-1-null mice, soluble recombinant PSGL-1 or anti-PSGL-1, as such treatments may have influenced normal lymphocyte recirculation by a heretofore unappreciated mechanism. This newly identified function of PSGL-1 may extend to other examples of chemokine interactions and possibly to some cytokines as well. Indeed, there have been several reports indicating anti-inflammatory effects of recombinant soluble PSGL-1 or neutralizing mAb to PSGL-1 that could not be explained by selectin antagonism[37–39].

METHODS

Chemokines. All chemokines were chemically synthesized 'in-house' with tBoc (tertiary butyloxycarbonyl) solid-phase chemistry. Chemokines were purified by high-performance liquid chromatography, and mass was confirmed by electrospray mass spectrometry[40]. Biotinylated CCL21 was produced by the coupling of biotinamidohexanoic acid *N*-hydroxysuccinimide ester (Sigma) to the N terminus of CCL21 before the 'deprotection' and refolding steps.

Mice. C57BL/6, PSGL-1-deficient C57BL/6 and P-selectin-deficient C57BL/6 mice were from the Jackson Laboratory. CD-1 mice were from Charles River Laboratories. The generation of C2GlcNAcT-1-deficient mice[20], CD43-deficient mice[41], E-selectin-deficient mice[42] and mice expressing green fluorescent protein (GFP) ubiquitously from the cytomegalovirus-enhancer chicken actin hybrid promoter[43] has been described. Mice deficient in both GlcNAc6ST-1 and GlcNAc6ST-2, mice deficient in both C2GlcNAcT-1 and PSGL-1, and mice transgenic for GFP and deficient in PSGL-1 were generated by intercrossing mice of the appropriate specific genotypes[15,44]. All mice were backcrossed at least eight generations on a C57BL/6 background. Mice were maintained in specific pathogen–free conditions and all animal experiments were done according to institutional guidelines and were approved by the Animal Care Committee of the University of British Columbia and the Institutional Animal Care and Use Committee of the University of California San Francisco.

Preparation of Fab fragments. Fab fragments of mAb 4RA10 (ref. 37) and rat IgG1 (eBioscience) were generated and purified with the ImmunoPure Fab Preparation Kit following the manufacturer's recommendations (Pierce). Fragments were concentrated and washed into PBS on a Centricon-10 (Millipore). Protein purity was assessed by nonreducing SDS-PAGE, followed by detection with Coomassie blue (GelCode Blue; Pierce). Protein concentration was determined by measurement of the absorbance at 280 nm.

***In vivo* homing assays with mAb blockade.** Lymphocyte-homing assays were done as described[15]. Mesenteric node lymphocytes from 6- to 10-week-old CD-1 mice were isolated and were labeled with 5 μM CMFDA

(5-chloromethylfluorescein diacetate; Molecular Probes). Cells (3×10^7) were mixed with 100 μg of mAb 4RA10 or rat IgG1 (eBioscience) in 200 μl of PBS. Fab fragments (25 μg) of mAb 4RA10 or rat IgG1 were used for Fab inhibition experiments. The mixture was injected into the tail veins of age-matched (12-week-old) wild-type mice (C57BL/6) and mice doubly deficient in GlcNAc6ST-1 and GlcNAc6ST-2. At 1 h after injection, mice were killed and SLOs were collected. Lymphocytes in these organs were 'teased out' with two 25-gauge needles. The fractional content of $CMFDA^+$ cells in lymphocyte suspensions was determined by flow cytometry (FACScan; Becton-Dickinson). For each suspension, 5×10^5 cells were analyzed and acquired with CellQuest software (Becton-Dickinson). Data were normalized for each mouse by division of the fractional value of $CMFDA^+$ cells by the mean of the fractional values for all of the wild-type mice in the experiment.

Cell preparation for *in vivo* homing assays with knockout mice and competitive transwell chemotaxis assays. Superficial cervical, brachial, inguinal, mesenteric and axillary lymph nodes were removed from age-matched donor mice and were dissociated into single-cell suspensions with a stainless steel sieve in RPMI medium (Gibco) containing 10% (vol/vol) FBS, 2 mM L-glutamine and 50 μM 2-mercaptoethanol and were kept at 4 °C. In some experiments, samples were depleted of B cells with anti–mouse IgG Dynabeads (Invitrogen). In experiments requiring 'concanavalin A blasts', cells were cultured for 4 d in complete RPMI medium with 2% (vol/vol) interleukin 2–containing media, conditioned by myeloma X.653 cells transfected with cDNA encoding mouse IL-2, and 4 μg/ml of concanavalin A. When cells were ready for use, they were washed, and viable cells were counted on a hemocytometer. Non-GFP^+ lymph node cells were labeled for 5 min at 25 °C with 0.2 μM CFDA-SE (5-(and-6)-carboxyfluorescein diacetate succinimidyl ester; Molecular Probes) in RPMI medium containing 10% (vol/vol) FCS or for 8 min at 37 °C with 8 μM Cell Tracker Orange (CTO; Molecular Probes) in Hank's balanced-salt solution (14185-052; Invitrogen Life Technologies). Immediately after being labeled, cells were washed once with RPMI medium containing 10% (vol/vol) FBS, then once with Hank's balanced-salt solution (Gibco). A ratio of 1:1 was determined by the cell count on the hemocytometer, then was verified by flow cytometry before injection. Cells were combined based on flow cytometry data. A final cell count was obtained with beads as described[41].

***In vivo* homing assays with knockout mice.** After 2×10^6 cells of each dye-labeled sample were combined and suspended in Hank's balanced-salt solution, they were injected intravenously into wild-type C57BL/6, P-selectin-deficient or E-selectin-deficient recipient mice, which were killed 1 h later in the same order in which they were injected. Peripheral blood, spleens, Peyer's patches and brachial, inguinal, mesenteric and axillary lymph nodes were collected and kept on ice. Peripheral blood was collected by perfusion with 2.5 mM EDTA in PBS and was added to a solution containing 2.5 mM EDTA and 4% (vol/vol) FBS in PBS. All lymph nodes were pooled, as were Peyer's patches. Spleens, lymph nodes and Peyer's patches were mechanically dissociated into single-cell suspensions into RPMI medium containing 10% (vol/vol) FBS. Peripheral blood and spleens were treated for 10 and 5 min, respectively, with red blood cell–lysis buffer. All cells were washed and resuspended three times with media. Subsets were determined with mAb to CD8 (CL8938B; clone CT-CD8b; Cedarlane), mAb to CD4 (553730; clone GK1.5; BD Pharmingen), mAb to CD44 (17-0441; clone IM7; eBiosciences) and mAb to B220 (553091; clone RA3-6B2; BD Pharmingen). CFDA-SE was detected in the FL1 channel and CTO was detected in the FL2 channel of the FACScan (Becton Dickinson). Flow cytometry data were analyzed with FlowJo (TreeStar) and Excel (Microsoft) software and were normalized to the results of wild-type mice.

Competitive transwell chemotaxis assay. Chemotaxis buffer (600 μl; RPMI medium, 100 mM HEPES, pH 7.2, and 0.5% (wt/vol) BSA) containing chemokine was added to the lower chamber of a transwell plate (Costar), followed by prewarming for a minimum of 1 h at 37 °C. GFP- or dye-labeled cells were transferred to chemotaxis buffer prewarmed to 37 °C and were resuspended at a density of 10×10^6 viable cells per ml. Prepared mixed cells (100 μl) were added to the upper transwell chamber, followed by incubation for 2–3 at 37 °C. In antibody inhibition experiments, 50 μl antibody was added to the upper transwell chamber first, followed by 50 μl of mixed cells at a density of 20×10^6 viable cells per ml. Migrated cells were quantified by flow cytometry (FACScan, Becton-Dickinson) and cell-counting beads as described[41]. Flow cytometry data were analyzed with FlowJo and Excel software. Absolute cell counts were normalized for differences in starting numbers and were adjusted relative to 'no-chemokine' controls.

PSGL-1–human IgG1 chimera. The cDNA encoding the 45 N-terminal amino acids of mature mouse PSGL-1 (primers: mPSGL-1_fw_ClaI, 5′-CCATCGA TGGGCAGGTGGTTGGGGATGACG-3′; mPSGL-1_45_rv_EcoRI, 5′ CCGGA ATTCCGGCACGGTGGTTGGCAGCTC-3′) and cDNA encoding the human IgG1 hinge, CH2 and CH3 domains (primers: hIgG_fw_EcoRI, 5′-CCGGAAT TCCGGACATGCCCACCGTGCCCA-3′; hIgG_rv_BamHI, 5′-CGCGGATCC GCGTCAGAGGCTCTTCTGCGT-3′) was amplified by PCR. The template for the IgG1 tag was a vector encoding human IgG1 (ref. 45). PCR products were cloned into the respective cloning sites of a pBluescriptII SK cloning vector. The insert was then cloned into a pMXpie expression vector containing the leader sequence of mouse CD43 followed by a Flag tag[46] using *Cla*I and *Not*I restrictions sites, respectively. The vector was transiently transfected into Chinese hamster ovary cells with Lipofectamin Plus (Invitrogen). After 48 h, supernatants were purified on a protein G column.

For binding assays, 400 ng to 25 ng of CCL21 and CXCL12 was dotted onto Hybond ECL nitrocellulose membranes (Amersham Biosciences). Membranes were blocked for 2 h with 5% (wt/vol) BSA in Tris-buffered saline and were then incubated for 2 h with 50 μg/ml of PSGL-1–IgG. For detection of binding, membranes were incubated for 1 h with anti–human IgG (Jackson Immuno-Research) and then were incubated for 1 h with Alexa Fluor 680–streptavidin (Molecular Probes). Membranes were analyzed with the Odyssey Infrared Imaging System (LI-COR).

Chemokine binding assays. Biotin-CCL21 (0.67 nmol) and 1.1 μg fluorescein isothiocyanate–streptavidin (BD Pharmingen) were mixed and were preincubated for 30 min in 30 μl chemotaxis buffer plus 2% (wt/vol) BSA, then were mixed with 1×10^6 lymphocytes in 70 μl chemotaxis buffer plus 0.5% (wt/vol) BSA, followed by incubation for 2 h at 37 °C. Cells were then washed once with 10% (vol/vol) FCS in PBS, and were stained for lymphocyte markers CD4, CD8 or B220. After 20 min of incubation, cells were washed twice in 10% (vol/vol) FCS in PBS and were analyzed with a FACSCalibur (Becton Dickinson).

Statistical analysis. Microsoft Excel was used for all statistical analyses. Statistical significance was determined by the two-tailed, unpaired Student's *t*-test; $\alpha = 0.05$ for all tests.

Note: Supplementary information is available on the Nature Immunology website.

ACKNOWLEDGMENTS

We thank R. Beavis for discussions; K.M. McNagny for critically reading the manuscript; P.D. Ziltener and M.J. Ford for technical assistance; J. Marth (University of California at San Diego) for C2GlcNAcT-1-deficient mice; D.C. Bullard (University of Alabama) for E-selectin-deficient mice; I. Weissman (Stanford University) for mice expressing GFP; G. McLean (University of Texas Health Sciences Center at Houston) for the vector encoding for human IgG1; and F. Melchers (Basel Institute of Immunology) for myeloma X.653 cells transfected with cDNA encoding mouse IL-2. Supported by the National Institutes of Health (R01GM57411 and R01GM23547 to S.D.R.), the Canadian Institutes for Health Research (J.S.M.; MOP-64267 and MOP-77552 to H.J.Z.) and Deutsche Forschungsgemeinschaft (S.N.)

AUTHOR CONTRIBUTIONS

J.S.M., H.J.Z. and K.U., S.D.R. independently discovered the PSGL-1 requirement for T cell homing; K.M.V. did the competitive homing assays; K.U. and M.S.S. did the mAb inhibition homing assays; M.J.W. designed and did the chemotaxis and CCL21 binding assays; S.N. contributed to the CCL21 binding studies; D.A.C. contributed to the experimental design of the competitive *in vivo* and *in vitro* studies; P.O. produced all chemokines; J.R.-N. provided anti-PSGL-1 and helped with the inhibition studies; H.J.Z. and S.D.R. supervised research and coordinated ongoing work; K.M.V. and H.J.Z. wrote the first draft of the manuscript; and all authors contributed to discussions and preparation of the manuscript.

COMPETING INTERESTS STATEMENT
The authors declare no competing financial interests.

Published online at http://www.nature.com/natureimmunology
Reprints and permissions information is available online at http://npg.nature.com/reprintsandpermissions

1. von Andrian, U.H. & Mempel, T.R. Homing and cellular traffic in lymph nodes. *Nat. Rev. Immunol.* **3**, 867–878 (2003).
2. Rosen, S.D. Ligands for L-selectin: homing, inflammation, and beyond. *Annu. Rev. Immunol.* **22**, 129–156 (2004).
3. Miyasaka, M. & Tanaka, T. Lymphocyte trafficking across high endothelial venules: dogmas and enigmas. *Nat. Rev. Immunol.* **4**, 360–370 (2004).
4. Forster, R. *et al.* CCR7 coordinates the primary immune response by establishing functional microenvironments in secondary lymphoid organs. *Cell* **99**, 23–33 (1999).
5. Gunn, M.D. *et al.* Mice lacking expression of secondary lymphoid organ chemokine have defects in lymphocyte homing and dendritic cell localization. *J. Exp. Med.* **189**, 451–460 (1999).
6. Weninger, W. & von Andrian, U.H. Chemokine regulation of naive T cell traffic in health and disease. *Semin. Immunol.* **15**, 257–270 (2003).
7. Campbell, J.J. & Butcher, E.C. Chemokines in tissue-specific and microenvironment-specific lymphocyte homing. *Curr. Opin. Immunol.* **12**, 336–341 (2000).
8. Lowe, J.B. Glycan-dependent leukocyte adhesion and recruitment in inflammation. *Curr. Opin. Cell Biol.* **15**, 531–538 (2003).
9. Okada, T. *et al.* Chemokine requirements for B cell entry to lymph nodes and Peyer's patches. *J. Exp. Med.* **196**, 65–75 (2002).
10. Tang, M.L., Steeber, D.A., Zhang, X.Q. & Tedder, T.F. Intrinsic differences in L-selectin expression levels affect T and B lymphocyte subset-specific recirculation pathways. *J. Immunol.* **160**, 5113–5121 (1998).
11. Gauguet, J.M., Rosen, S.D., Marth, J.D. & von Andrian, U.H. Core 2 branching β1,6-*N*-acetylglucosaminyltransferase and high endothelial cell *N*-acetylglucosamine-6-sulfotransferase exert differential control over B- and T-lymphocyte homing to peripheral lymph nodes. *Blood* **104**, 4104–4112 (2004).
12. Sackstein, R. The lymphocyte homing receptors: gatekeepers of the multistep paradigm. *Curr. Opin. Hematol.* **12**, 444–450 (2005).
13. Ley, K. The role of selectins in inflammation and disease. *Trends Mol. Med.* **9**, 263–268 (2003).
14. Rossi, F.M. *et al.* Recruitment of adult thymic progenitors is regulated by P-selectin and its ligand PSGL-1. *Nat. Immunol.* **6**, 626–634 (2005).
15. Uchimura, K. *et al.* A major class of L-selectin ligands is eliminated in mice deficient in two sulfotransferases expressed in high endothelial venules. *Nat. Immunol.* **6**, 1105–1113 (2005).
16. Kawashima, H. *et al.* *N*-acetylglucosamine-6-*O*-sulfotransferases 1 and 2 cooperatively control lymphocyte homing through L-selectin ligand biosynthesis in high endothelial venules. *Nat. Immunol.* **6**, 1096–1104 (2005).
17. Ley, K. & Kansas, G.S. Selectins in T-cell recruitment to non-lymphoid tissues and sites of inflammation. *Nat. Rev. Immunol.* **4**, 325–335 (2004).
18. Spertini, O., Cordey, A.S., Monai, N., Giuffre, L. & Schapira, M. P-selectin glycoprotein ligand 1 is a ligand for L-selectin on neutrophils, monocytes, and CD34+ hematopoietic progenitor cells. *J. Cell Biol.* **135**, 523–531 (1996).
19. Martinez, M. *et al.* Regulation of PSGL-1 interactions with L-selectin, P-selectin, and E-selectin: role of human fucosyltransferase-IV and -VII. *J. Biol. Chem.* **280**, 5378–5390 (2005).
20. Ellies, L.G. *et al.* Core 2 oligosaccharide biosynthesis distinguishes between selectin ligands essential for leukocyte homing and inflammation. *Immunity* **9**, 881–890 (1998).
21. Pilkington, K.R., Clark-Lewis, I. & McColl, S.R. Inhibition of generation of cytotoxic T lymphocyte activity by a CCL19/macrophage inflammatory protein (MIP)-3β antagonist. *J. Biol. Chem.* **279**, 40276–40282 (2004).
22. Hirata, T. *et al.* Human P-selectin glycoprotein ligand-1 (PSGL-1) interacts with the skin-associated chemokine CCL27 via sulfated tyrosines at the PSGL-1 amino terminus. *J. Biol. Chem.* **279**, 51775–51782 (2004).
23. Fukuda, M. Leukosialin, a major O-glycan-containing sialoglycoprotein defining leukocyte differentiation and malignancy. *Glycobiology* **1**, 347–356 (1991).
24. Baekkevold, E.S. *et al.* The CCR7 ligand elc (CCL19) is transcytosed in high endothelial venules and mediates T cell recruitment. *J. Exp. Med.* **193**, 1105–1112 (2001).
25. Scimone, M.L. *et al.* CXCL12 mediates CCR7-independent homing of central memory cells, but not naive T cells, in peripheral lymph nodes. *J. Exp. Med.* **199**, 1113–1120 (2004).
26. Yoshida, R. *et al.* Secondary lymphoid-tissue chemokine is a functional ligand for the CC chemokine receptor CCR7. *J. Biol. Chem.* **273**, 7118–7122 (1998).
27. Hirose, J., Kawashima, H., Yoshie, O., Tashiro, K. & Miyasaka, M. Versican interacts with chemokines and modulates cellular responses. *J. Biol. Chem.* **276**, 5228–5234 (2001).
28. Frenette, P.S. *et al.* P-Selectin glycoprotein ligand 1 (PSGL-1) is expressed on platelets and can mediate platelet-endothelial interactions *in vivo*. *J. Exp. Med.* **191**, 1413–1422 (2000).
29. Loetscher, M. *et al.* Chemokine receptor specific for IP10 and mig: structure, function, and expression in activated T-lymphocytes. *J. Exp. Med.* **184**, 963–969 (1996).
30. Willimann, K. *et al.* The chemokine SLC is expressed in T cell areas of lymph nodes and mucosal lymphoid tissues and attracts activated T cells via CCR7. *Eur. J. Immunol.* **28**, 2025–2034 (1998).
31. Xia, L. *et al.* N-terminal residues in murine P-selectin glycoprotein ligand-1 required for binding to murine P-selectin. *Blood* **101**, 552–559 (2003).
32. Li, F. *et al.* Visualization of P-selectin glycoprotein ligand-1 as a highly extended molecule and mapping of protein epitopes for monoclonal antibodies. *J. Biol. Chem.* **271**, 6342–6348 (1996).
33. Moore, K.L. *et al.* P-selectin glycoprotein ligand-1 mediates rolling of human neutrophils on P-selectin. *J. Cell Biol.* **128**, 661–671 (1995).
34. Hidari, K.I., Weyrich, A.S., Zimmerman, G.A. & McEver, R.P. Engagement of P-selectin glycoprotein ligand-1 enhances tyrosine phosphorylation and activates mitogen-activated protein kinases in human neutrophils. *J. Biol. Chem.* **272**, 28750–28756 (1997).
35. Ba, X., Chen, C., Gao, Y. & Zeng, X. Signaling function of PSGL-1 in neutrophil: tyrosine-phosphorylation-dependent and c-Abl-involved alteration in the F-actin-based cytoskeleton. *J. Cell. Biochem.* **94**, 365–373 (2005).
36. Galkina, E. *et al.* L-selectin shedding does not regulate constitutive T cell trafficking but controls the migration pathways of antigen-activated T lymphocytes. *J. Exp. Med.* **198**, 1323–1335 (2003).
37. Rivera-Nieves, J. *et al.* Critical role of endothelial P-selectin glycoprotein ligand 1 in chronic murine ileitis. *J. Exp. Med.* **203**, 907–917 (2006).
38. Hicks, A.E., Nolan, S.L., Ridger, V.C., Hellewell, P.G. & Norman, K.E. Recombinant P-selectin glycoprotein ligand-1 directly inhibits leukocyte rolling by all 3 selectins *in vivo*: complete inhibition of rolling is not required for anti-inflammatory effect. *Blood* **101**, 3249–3256 (2003).
39. Sumariwalla, P.F., Malfait, A.M. & Feldmann, M. P-selectin glycoprotein ligand 1 therapy ameliorates established collagen-induced arthritis in DBA/1 mice partly through the suppression of tumour necrosis factor. *Clin. Exp. Immunol.* **136**, 67–75 (2004).
40. Clark-Lewis, I., Mattioli, I., Gong, J.H. & Loetscher, P. Structure-function relationship between the human chemokine receptor CXCR3 and its ligands. *J. Biol. Chem.* **278**, 289–295 (2003).
41. Carlow, D.A., Corbel, S.Y. & Ziltener, H.J. Absence of CD43 fails to alter T cell development and responsiveness. *J. Immunol.* **166**, 256–261 (2001).
42. Bullard, D.C. *et al.* Infectious susceptibility and severe deficiency of leukocyte rolling and recruitment in E-selectin and P-selectin double mutant mice. *J. Exp. Med.* **183**, 2329–2336 (1996).
43. Corbel, S.Y. *et al.* Contribution of hematopoietic stem cells to skeletal muscle. *Nat. Med.* **9**, 1528–1532 (2003).
44. Merzaban, J.S., Zuccolo, J., Corbel, S.Y., Williams, M.J. & Ziltener, H.J. An alternate core 2 β1,6-*N*-acetylglucosaminyltransferase selectively contributes to P-selectin ligand formation in activated CD8 T cells. *J. Immunol.* **174**, 4051–4059 (2005).
45. McLean, G.R., Nakouzi, A., Casadevall, A. & Green, N.S. Human and murine immunoglobulin expression vector cassettes. *Mol. Immunol.* **37**, 837–845 (2000).
46. Drew, E., Merzaban, J.S., Seo, W., Ziltener, H.J. & McNagny, K.M. CD34 and CD43 inhibit mast cell adhesion and are required for optimal mast cell reconstitution. *Immunity* **22**, 43–57 (2005).

Reprint from

Naoyuki Taniguchi, Akemi Suzuki, Yukishige Ito, Hisashi Narimatsu,

Toshisuke Kawasaki, Sumihiro Hase (Eds.)

Experimental Glycoscience

Glycobiology

Springer

N-acetylglucosamine-6-*O*-sulfotransferases

Kenji Uchimura,[1] Takashi Muramatsu[2]

Introduction

N-acetylglucosamine-6-*O*-sulfotransferase (GlcNAc6ST) transfers a sulfate group from PAPS to an *N*-acetylglucosamine residue, which is usually located at the non-reducing end of glycoconjugates. It is important to note that sulfation proceeds the elongation of the glycan chain. This enzyme is involved in the synthesis of keratan sulfate and sialyl 6-sulfo Lewis X, which is present on the luminal surface of the high endothelial venule (HEV) of lymph nodes. So far, five isozymes of GlcNAc6ST have been identified in humans (Table 1). They share about 30% sequence identity, and have the configuration of type II transmembrane proteins, a feature typical of Golgi-located enzymes.

The sulfate group is transferred only to C-6 of *N*-acetylglucosamine by GlcNAc6ST-1, the first cloned enzyme, which was shown by a biochemical analysis of the product (Uchimura et al. 1998). Convenient substrates to assay GlcNAc6STs are oligosaccharides with an *N*-acetylglucosamine terminus, and radioactively labeled PAPS as the sulfate donor. Usually, the product of the enzymatic reaction is separated from PAPS by high-performance liquid chromatography or thin-layer chromatography. The latter procedure is useful for assaying a large number of samples (Uchimura et al. 2002). Substrate specificities of GlcNAc6STs assayed in vitro are not dramatically different from each other. However, among GlcNAc6ST-1, -2, and -3, only GlcNAc6ST-2 can act on core 3 structure (Galβ1-3GalNAc) (Uchimura et al. 2002). As reported by de Graffenried and Bertozzi, Golgi localization of GlcNAc6STs is different: GlcNA6ST-1 is confined to the trans-Golgi network, GlcNAc6ST-3 is confined to the early secretory pathway, and GlcNAc6ST-2 is distributed throughout the Golgi. This difference in localization influences enzymatic activities observed in intact cells.

Comments

Important roles played by GlcNAc6STs have been revealed especially by employing genetical approaches. Sialyl 6-sulfo Lewis X is a ligand structure of L-selectin, which

[1] Section of Pathophysiology and Neurobiology, Department of Alzheimer's Disease Research, National Institute for Longevity Sciences (NILS), 36-3 Gengo, Morioka, Obu, Aichi 474-8522, Japan
Phone: +81-562-46-2311, Fax: +81-562-46-3157
E-mail: arumihcu@nils.go.jp

[2] Department of Health Science, Faculty of Psychological and Physical Science, Aichi Gakuin University, 12 Araike, Iwasaki-cho, Nisshin, Aichi 470-0195, Japan
Phone: +81-561-73-1111, Fax: +81-561-73-1142
E-mail: tmurama@dpc.aichi-gakuin.ac.jp

Table 1 *N*-acetylglucosamine-6-sulfotransferases

Name	Other abbreviated names	Gene name	Map	Accession No.	Major sites of expression	PubMed ID No. for key references
GlcNAc6ST-1		*CHST2*	3q24	NM-004267	Multiple tissues	9712885, 10200296, 11726653, 12855678, 15175329, 15220337, 15728736, 1622785, 16227986, 16624895, 16772045
GlcNAc6ST-2	LSST HEC-GLCNAcST	*CHST4*	16q22.3	NM-005769	HEV	10330415, 10435581, 11520459, 11726653, 12107080, 12855678, 14597732, 16227985, 16227986, 16772045, 16897186
GlcNAc6ST-3	I-GlcNAcST	*CHST5*	16q22	NM-024533	Intestine, cornea	10491328, 11278593, 11726653, 12855678, 16938851
GlcNAc6ST-4	C6ST-2	*CHST7*	Xp11.3	NM-019886	Multiple tissues	10781596, 10913333, 10956661
GlcNAc6ST-5	C-GlcNAcST	*CHST6*	16q22	NM-021615	Cornea	11017086, 11278593, 15013869

Gene name, chromosomal location, and accession No. are those of human enzymes

regulates the initial step of lymphocyte homing to lymph nodes by inducing the rolling of lymphocytes on the luminal surface of HEV. GlcNAc6ST-2 is preferentially expressed in HEV, and GlcNAc6ST-1 is expressed in many tissues including HEV. In GlcNAc6ST-2-deficient mice, lymphocyte homing to peripheral lymph nodes is reduced to 50–60% of that observed in wild-type mice. However, in double knockout (DKO) mice, deficient in both GlcNAc6ST-1 and -2, the value is reduced to 25%, indicating that both enzymes are involved in the synthesis of L-selectin ligand (Kawashima et al. 2005; Uchimura et al. 2005). The complete loss of sialyl 6-sulfo Lewis X structure from HEV of DKO mice is indicated by biochemical and immunohistochemical analyses. In HEV of DKO mice, the rolling of lymphocytes is still observed, but the rolling velocity is greatly increased. Thus, sialyl Lewis X structure without GlcNAc6-sulfation is sufficient to induce a minimum level of rolling, and its GlcNAc-6-sulfation normalizes rolling by decreasing the rolling velocity.

GlcNA6ST-5 is expressed in the cornea and is involved in the synthesis of keratan sulfate. Null mutation of GlcNAc6ST-5 in human leads to macular corneal dystrophy type I and II (Akama et al. 2000). GlcNAc6ST-3 is closely related to GlcNAc6ST-5. Hayashida et al. have revealed that knockout mice deficient in GlcNAc6ST-3 lack highly sulfated keratan sulfate in the cornea and have thinner corneas compared to wild-type mice. The collagen fibrillar architecture is markedly altered in the cornea of the mutant mice. Zhang et al. have shown that GlcNAc6ST-1 is involved in the synthesis of highly sulfated keratan sulfate in the brain. Synthesis of highly sulfated keratan sulfate is

induced upon brain injury. In GlcNAc6ST-1 knockout mice, this induction is impaired, and glial scar formation, which inhibits repair of the brain, is suppressed.

Upregulation of GlcNAc6STs under pathological conditions is a subject of significant interest. The GlcNAc6ST-2 level is increased in mucinous adenocarcinoma of the colon, and in chemotherapy-resistant ovarian adenocarcinoma. Expression of GlcNAc6ST-1 and -2 is increased in the synovium of mice upon collagen-induced arthritis, a model of rheumatoid arthritis.

Protocol: GlcNAc-6-O-sulfotransferase Assay

Microsomal fractions in mammalian cell lines that are transfected with expression plasmids encoding GlcNAc-6-*O*-sulfotransferases are used as enzymes. Various oligosaccharides derived from N-linked or O-linked glycans and keratan sulfate are applicable to the assay described here. Oligosaccharide substrates tested are GlcNAcβ1-3Galβ1-4GlcNAc, GlcNAcβ1-6Man-*O*-methyl, GlcNAcβ1-2Man, GlcNAcβ-6[Galβ1-3]GalNAc-*p*-nitrophenyl and GlcNAcβ1-3GalNAc-*p*-nitrophenyl. Thin-layer chromatography (TLC) is employed to handle a large number of samples.

1. The standard reaction mixture in a 1.5 mL tube contains 1 μmol Tris–HCl, pH 7.5, 0.2 μmol $MuCl_2$, 0.04 μmol adenosine 5′-monophosphate, 2 μmol sodium fluoride, 20 μmol oligosaccharides, 150 pmol [^{35}S]-3′phosphoadenosine 5′-phosphosulfate (PAPS) (1.5×10^6 cpm), 0.05% of Triton-X and 5 μL of enzymes in a final volume of 20 μL.
2. Incubate the tube containing the reaction mixture at 30°C for 1 h.
3. Aliquots of 2 μL of the reaction mixture are applied to TLC plates. The plates are precoated with 0.1-mm thick cellulose.
4. Develop the plates with a developing solvent, ethanol/pyridine/*n*-butyl alcohol/water/acetic acid (100:10:10:30:3, by volume).
5. End the development when the solvent front reaches to the top of the plates. The ^{35}S-labeled oligosaccharides migrate faster than [^{35}S]-PAPS.

The radioactivity of the ^{35}S-labeled oligosaccharides is visualized and measured using a BAS2000 bioimaging analyzer.

References

Akama TO, Nishida K, Nakayama J, Watanabe H, Ozaki K, Nakamura T, Dota A, Kawasaki S, Inoue Y, Maeda N, Yamamoto S, Fujiwara T, Thonar EJ, Shimomura Y, Kinoshita S, Tanigami A, Fukuda MN (2000) Macular corneal dystrophy type I and type II are caused by distinct mutations in a new sulphotransferase gene. Nat Genet 26:237–241

Kawashima H, Petryniak B, Hiraoka N, Mitoma J, Huckaby V, Nakayama J, Uchimura K, Kadomatsu K, Muramatsu T, Lowe JB, Fukuda M (2005) *N*-acetylglucosamine-6-*O*-sulfotransferases 1 and 2 cooperatively control lymphocyte homing through L-selectin ligand biosynthesis in high endothelial venules. Nat Immunol 6:1096–1104

Uchimura K, Muramatsu H, Kadomatsu K, Fan QW, Kurosawa N, Mitsuoka C, Kannagi R, Habuchi O, Muramatsu T (1998) Molecular cloning and characterization of an *N*-acetylglucosamine-6-*O*-sulfotransferase. J Biol Chem 273:22577–22583

Uchimura K, El-Fasakhany FM, Hori M, Hemmerich S, Blink SE, Kansas GS, Kanamori A, Kumamoto K, Kannagi R, Muramatsu T (2002) Specificities of *N*-acetylglucosamine-6-*O*-sulfotransferases in relation to L-selectin ligand synthesis and tumor-associated enzyme expression. J Biol Chem 277:3979–3984

Uchimura K, Gauguet JM, Singer MS, Tsay D, Kannagi R, Muramatsu T, von Andrian UH, Rosen SD (2005) A major class of L-selectin ligands is eliminated in mice deficient in two sulfotransferases expressed in high endothelial venules. Nat Immunol 11:1105–1113

Reprint from

Naoyuki Taniguchi, Akemi Suzuki, Yukishige Ito, Hisashi Narimatsu,

Toshisuke Kawasaki, Sumihiro Hase (Eds.)

Experimental Glycoscience

Glycobiology

Springer

Sulfotransferases

Takashi Muramatsu[1], **Kenji Uchimura**[2]

Introduction

Molecular cloning has been accomplished for a large number of carbohydrate sulfotransferases. The majority of them are involved in the synthesis of glycosaminoglycans such as heparan sulfate, chondroitin sulfate, and keratan sulfate (Habuchi et al. 2006), whereas some of them play roles in formation of glycans in glycoproteins or glycolipids. Increasing numbers of carbohydrate sulfotransferases have been knocked out in mice to understand the role of sulfate groups more precisely (Table 1). Interestingly, all knockout mice exhibit phenotypes, underlining the physiological importance of carbohydrate sulfation.

Comments

The first carbohydrate sulfotransferase knocked out was heparan sulfate 2-O-sulfotransferase. Inactivation of the gene by Gene trap leads to neonatal death in mice due to failure of kidney formation (Bullock et al. 1998). The striking phenotype gave convincing evidence that heparan sulfate plays important roles in mammalian development.

Heparan sulfate/heparin *N*-deacetylase/*N*-sulfotransferase (NDST) catalyzes both the deacetylation and sulfation of an amino group in *N*-acetylglucosamine. NDST1 is involved in the synthesis of heparan sulfate, and NDST-2 in the synthesis of heparin. The action of NDST usually precedes the action of other sulfotransferases. However, in embryonic stem cells derived from NDST1 and NDST2 double knockout mice, which lack *N*-sulfated glucosamine, heparan sulfate with 6-sulfated *N*-acetylglucosamine was detected, indicating that the 6-sulfation step, which does not require *N*-sulfation, is present (Holmborn et al. 2004). Reflecting the physiological importance of heparan sulfate, NDST1 knockout mice die at the neonatal stage (Ringvall et al. 2000). Conditional knockout at a restricted tissue is required to understand the precise role of heparan sulfate chain in a physiological process (Wang et al. 2005).

N-acetylglucosamine-6-*O*-sulfotransferases (GlcNAc6STs) are involved in the synthesis of both L-selectin ligands and keratan sulfate. Decreased lymphocyte homing in GlcNAc6ST deficient mice is due to the impaired synthesis of L-selectin ligand and other phenotypes are due to failure in the synthesis of highly-sulfated keratan sulfate. In vivo lymphocyte homing assay is shown as a protocol. Further information concerning the

[1] Department of Health Science, Faculty of Psychological and Physical Science, Aichi Gakuin University, 12 Araike, Iwasaki-cho, Nisshin, Aichi 470-0195, Japan
Phone: +81-561-73-1111, Fax: +81-561-73-1142
E-mail: tmurama@dpc.aichi-gakuin.ac.jp

[2] Section of Pathophysiology and Neurobiology, Department of Alzheimer's Disease Research, National Institute for Longevity Sciences (NILS), 36-3 Gengo, Morioka, Obu, Aichi 474-8522, Japan
Phone: +81-562-46-2311, Fax: +81-562-46-3157
E-mail: arumihcu@nils.go.jp

Table 1 List of knockout of carbohydrate sulfotransferases

Name of enzymes	Methods	Phenotypes	PubMed ID No. of key references
Heparan sulfate/ heparin *N*-deacetylase/ *N*-sulfotransferase-1	KO, conditional KO	Neonatal death; disturbed Calcium ion kinetics in myotube; cerebral hypoplasia and craniofacial defects; impaired neutrophil infiltration	10852901, 12692154, 15292174, 15319440, 16020517, 16056228
Heparan sulfate/ heparin *N*-deacetylase/ *N*-sulfotransferase-2	KO	Abnormal mast cells	10466726, 10466727
Heparan sulfate 2-*O*-sulfotransferase	Gene trap	Neonatal death due to renal agenesis; impaired retinal axon guidance	9637690, 16807321
Heparan sulfate 3-*O*-sulfotransferase-1	KO	Normal hemostasis; genetic background-specific lethality and intrauterine growth retardation	12671048
Heparan sulfate 6-*O*-sulfotransferase-1	Gene trap, KO	Impaired retinal axon guidance; Abnormalities in fetal microvessels	16807321, 17405882
Chondroitin 4-sulfotransferese	Gene trap	Severe chondrodysplasia	16079159
Chondroitin 6-sulfotransferese	KO	Decreased naïve T lymphocytes in the spleen of young mice	11696535
N-Acetylglucosamine-6-*O*-sulfotransferase-1	KO	Decreased lymphocyte homing; suppression of glial scar formation in the injured brain	15175329, 16227985, 16227986, 16624895
N-Acetylglucosamine-6-*O*-sulfotransferase-2	KO	Decreased lymphocyte homing	11520459, 14597732, 16227985, 16227986
N-Acetylglucosamine-6-*O*-sulfotransferase-3	KO	Thin cornea	16938851
HNK-1 sulfotransferase	KO	Alterations in synaptic efficacy, spatial learning and memory; reduced extracellular space in the brain	12213450, 12358771, 16262627
Cerebroside sulfotransferase	KO	Abnormalities in paranodal junctions; male sterility; impaired neutrophil infiltration	11917099, 12151530, 14583626, 15659616

phenotype of GlcNAc6ST knockout mice is provided in the section on GlcNAc6STs. Among five isozymes of GlcNAc6STs, three enzymes have been knocked out. Among isozymes of heparan sulfate 3-*O*-sulfotransferases, so far, knockout of only one enzyme has been published. This is also true for heparan sulfate 6-*O*-sulotransferases.

Cerebroside sulfotransferase is involved in the formation of both sulfatide (HSO3-3-galactosyl ceramide) and seminolipid (HSO3-3-monogalactosylacylglycerol). The neurological phenotype observed in cerebroside sulfotransferase knockout mice is ascribed to the lack of sulfatide, and male sterility in these mice is due to the impaired synthesis of seminolipid.

Protocol: In Vivo Lymphocyte Homing Assay

Lymphocytes circulate between the blood and the lymphoid organs. Lymphocyte homing to lymph nodes is initiated by the binding of L-selectin to its ligands. A major class of L-selectin ligands in lymphocyte homing is sialy 6-sulfo Lewis X. GlcNAc-6-O-sulfation is essential for the ligand activity. To assess the activity of homing ligand, an in vivo assay of lymphocyte homing is utilized. Lymphocyte donors and recipients in the assay described here are adult mice. Flow cytometry is used to quantify homing of lymphocytes to lymph nodes.

1. Dissect out mesenteric lymph nodes of 5- to 10-week-old CD-1 mice and place them in phosphate buffered saline (PBS).
2. Mush the nodes with two slide glasses to have single-cell suspensions in PBS.
3. Filter suspensions through a nylon cell strainer (40 μm pore size).
4. Metabolically label filtered cells with 5 μM 5-chloromethylfluorescein diacetate (CMFDA) at 37°C for 30 min.
5. Inject the cells (1.7×10^7 in 100 μl PBS/mouse) into tail veins of 8- to 10-week-old mice.
6. One hour after injection, kill the mice and dissect out peripheral lymph nodes, mesenteric lymph nodes, Peyer's patches, and spleen.
7. Create single-cell suspensions of these organs in PBS by teasing with 23-gauge needles.
8. Determine the fraction of CMFDA-labeled cells in suspensions by flow cytometry (5×10^5 cells per organ).
9. Acquire and analyze data with CellQuest software.

References

Bullock SL, Fletcher JM, Beddington RS, Wilson VA (1998) Renal agenesis in mice homozygous for a gene trap mutation in the gene encoding heparan sulfate 2-sulfotransferase. Genes Dev 12:1894–1906

Habuchi H, Habuchi O, Uchimura K, Kimata K, Muramatsu T (2006) Determination of substrate specificity of sulfotransferases and glycosyltransferases (proteoglycans). Methods Enzymol 416: 225–243

Holmborn K, Ledin J, Smeds E, Eriksson I, Kusche-Gullberg M, Kjellen L (2004) Heparan sulfate synthesized by mouse embryonic stem cells deficient in NDST1 and NDST2 is 6-O-sulfated but contains no N-sulfate groups. J Biol Chem 279:42355–42358

Ringvall M, Ledin J, Holmborn K, van Kuppevelt T, Ellin F, Eriksson I, Olofsson AM, Kjellen L, Forsberg E (2000) Defective heparan sulfate biosynthesis and neonatal lethality in mice lacking N-deacetylase/N-sulfotransferase-1. J Biol Chem 275:25926–25930

Wang L, Fuster M, Sriramarao P, Esko JD (2005) Endothelial heparan sulfate deficiency impairs L-selectin- and chemokine-mediated neutrophil trafficking during inflammatory responses. Nat Immunol 6:902–910

シリーズ最新医学講座・I　糖鎖と臨床検査・4

セレクチンと糖鎖

内村　健治

臨　床　検　査
第52巻　第4号 別刷
2008年4月15日　発行

医学書院

セレクチンと糖鎖

内村健治[1)]

KEYWORDS リンパ球，ホーミング，炎症，硫酸化

はじめに

リンパ球のリンパ節へのホーミングおよび白血球の末梢炎症部位への血行性移入は，1991年に提唱された多段階の分子シグナルによって厳密に制御されている(**図1**)[1,2]．すなわち，ターゲットとなる組織の血管内で血液中を流れる細胞は，セレクチンとその認識リガンドである細胞表面糖鎖の蛋白質-糖鎖の比較的弱い相互作用を利用し，血管内皮細胞上でローリングと呼ばれる現象を示し流速を減少させる(第1段階)．その後，内皮細胞上に提示されたケモカインとローリング細胞上のケモカイン受容体が結合し，ローリング細胞に活性化シグナルが入る(第2段階)．このシグナルがローリング細胞上のインテグリンを活性化し，内皮細胞上の細胞接着分子との蛋白質-蛋白質の結合を利用し強固な接着を引き起こす(第3段階)．最終的に細胞は，血管内皮細胞層をすり抜けて血管外遊走し組織内へ移入する(第4段階)．本稿では，この多段階モデルの最初のステップであるセレクチンとそのリガンド糖鎖について述べる．ケモカインのシグナル機構，およびインテグリンの活性化については他の総説[3)]に詳しい．

セレクチン

セレクチンファミリーにはL-セレクチン(CD62L)，P-セレクチン(CD62P)，E-セレクチン(CD62E)の3つのメンバーが存在する(**表1**)．これらセレクチン分子はN末端細胞外領域にカルシウム依存性レクチン様ドメインを持つ．L-セレクチンは多くの白血球の細胞表面で発現され，リンパ球のリンパ節へのホーミングに重要である．P-セレクチンは血小板のa顆粒および内皮細胞のWeibel-Palade小体に存在し，炎症性刺激により数分でそれぞれ細胞表面へ発現される．P-セレクチンのリガンドとして多くの白血

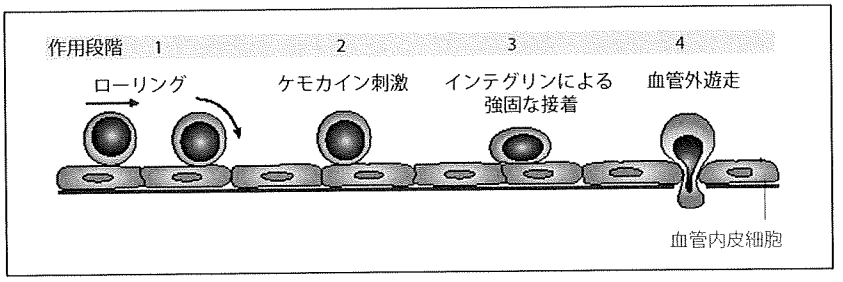

図1 白血球血行性組織内浸潤の多段階モデル 〔文献1)より一部改変して引用〕
セレクチンとその認識リガンドである細胞表面糖鎖の蛋白質-糖鎖分子相互作用は第一段階であるローリングに重要．本文参照．

1) UCHIMURA Kenji 国立長寿医療センター研究所・室長

表1　セレクチンファミリーとその発現様式

分子名	他の文献における命名	遺伝子名	おもな発現細胞	細胞表面発現様式
L-セレクチン (CD62L)	Leu8, gp90MEL, mLHR, TQ-1, Lam-1, Lecam-1, DREG-56	SELL	リンパ球, 単球, 好中球	恒常的に細胞表面に発現 細胞刺激により ADAM17 で shedding される
P-セレクチン (CD62P)	PAD GEM, GMP-140	SELP	血小板, 血管内皮細胞	ヒスタミンなどによりアルファ顆粒(血小板)Weibel-Palade 小体(血管内皮)内に貯留されたものが数分で細胞表面に発現 サイトカイン刺激により数時間で発現
E-セレクチン (CD62E)	ELAM-1	SELE	血管内皮細胞	サイトカイン刺激により数時間で発現

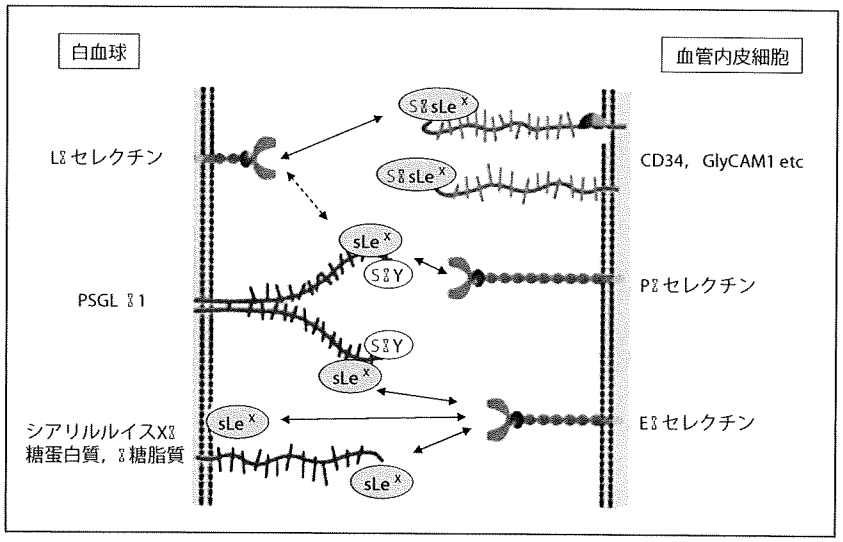

図2　白血球細胞表面および血管内皮細胞表面に発現されるセレクチンとそのリガンド分子　〔文献2)より一部改変して引用〕
L-セレクチンはシアロムチン糖蛋白質糖鎖の硫酸基修飾されたシアリルルイスX構造(S-sLeX)を認識する．P-セレクチンはPSGL-1分子の硫酸化チロシン残基(S-Y)とシアリルルイスX(sLe^X)の複合体を認識する．E-セレクチンは主に糖蛋白質や糖脂質糖鎖のシアリルルイスX構造を認識する．

球に発現されるPSGL-1(CD162)が知られている．PSGL-1分子N末端の硫酸化チロシン残基とシアリルルイスX糖鎖[4]の複合体をP-セレクチンは認識する(**図2**)[5]．E-セレクチンは，炎症性サイトカインにより内皮細胞での発現が誘導され，その細胞表面に提示される．E-セレクチンの主な認識決定構造は，シアリルルイスX様糖鎖であると考えられる．この糖鎖構造を持つ細胞表面分子は多く報告されており，PSGL-1，CD44，糖脂質がE-セレクチンリガンド分子として働くことが知られている(**図2**)[2]．

セレクチンと白血球のローリング

ナイーブリンパ球が末梢のリンパ節へホーミングする際，リンパ球表面のL-セレクチンとリンパ節内の高内皮細静脈(high endothelial venules：HEV)[6]に発現されるその硫酸化糖鎖リガンドとの分子相互作用により，ローリングが媒介される(**図2**)．ナイーブリンパ球は微小絨毛突起(mi-